



## **Tests on bolted steel angles in compression with varying end support conditions**

Markus Kettler<sup>1</sup>, Gerit Lichtl<sup>2</sup>, Harald Unterweger<sup>3</sup>

### **Abstract**

Structural steel angles are often used as bracing members in buildings or in lattice transmission towers. Bolted end-connections of single steel angles allow for easy fabrication and quick erection, but induce additional bending moments due to the eccentric load introduction. This leads to a complex load carrying behavior, especially for members in compression. This causes a decrease in capacity compared to the case of a simply supported column with centric loading for smaller slenderness ratios. For larger slenderness ratios the beneficial effect of end restraints is assumed to compensate this drawback. Current design standards account for these effects via modified effective slenderness ratios resulting in significantly different predictions for the member capacities according to the individual regulations.

The paper presents execution and results of a test series on single steel angles in compression with varying end support conditions and slenderness ratios. In total 27 specimens with one-bolt and two-bolt connections are tested. Three different boundary conditions on both ends are investigated: Boundary condition 1 (BC1) is a clamped support with all rotational degrees of freedom restraint at the member's ends. BC2 is a knife edge support that allows only for rotations about the axis parallel to the connected leg. BC3 is a fully hinged support with only the rotation about the longitudinal axis restraint. Accompanying to the results of the member tests, imperfection measurements and results of material tests are presented in order to allow for comparison with American and European design standards.

The comparison of test results shows a significant difference in the compression member capacity between clamped and hinged support conditions. This difference is even more pronounced than the difference between one-bolt and two-bolt connections – a state of affairs that is either not, or only insufficiently, reflected in current design code regulations.

### **1. Introduction**

The load carrying behavior of single-angle steel members in compression is rather complex, especially if the end connections are realized via bolted connections. Therefore, several

---

<sup>1</sup> Assistant Professor, Graz University of Technology – Austria, <kettler@TUGraz.at>

<sup>2</sup> Graduate Student, Graz University of Technology – Austria, <lichtl@student.tugraz.at>

<sup>3</sup> Professor, Graz University of Technology – Austria, <h.unterweger@TUGraz.at>

experimental test campaigns have been conducted in the past in order to investigate this subject. Since the main focus of the current paper is on hot-rolled angle sections, the following overview is limited to this section type (i.e. cold-formed angle sections are not covered), which are also not susceptible to local buckling.

Before giving an overview of the experimental tests in literature, Fig. 1 presents a comparison of the nominal compressive strength of single-angle members for bolted connections with minimum two bolts in the connected leg according to the relevant design codes for steel buildings of Europe (EN 1993-1-1), U.S.A. (AISC 360-16) and Canada (CSA S16-14). The embedded sketch of a hot-rolled angle section illustrates the eccentric load introduction, leading to a decrease in capacity compared to the case of a centrally loaded, simply supported column (member capacity based on buckling curve b for EN 1993-1-1) for smaller slenderness ratios, according to all three design codes. Note that the relevant buckling curves in AISC 360-16 and CSA S16-14 for the centrally loaded simply supported member are approximately the same as in EN 1993-1-1. The beneficial effect of end restraints can also clearly be seen for larger slenderness ratios.

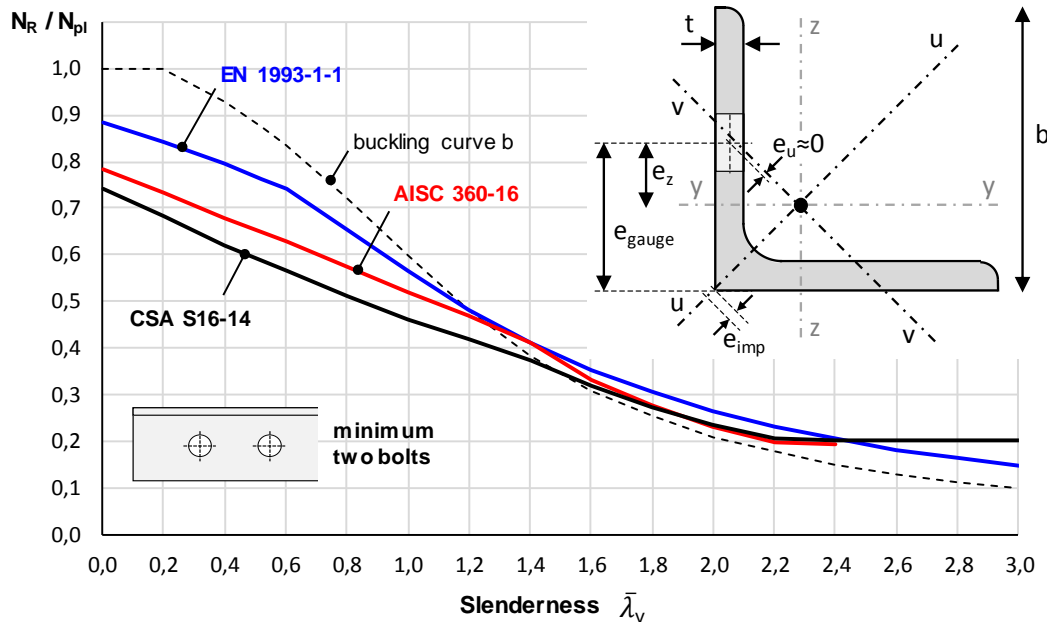


Figure 1: Comparison of nominal compressive strength of single-angle members for bolted connections with minimum two bolts

One of the first large test series was carried out in 1974 at laboratories in England, Spain and Germany (C.I.G.R.E. (1974)). In total 153 single-angle steel members (104 with two-bolt connections and 49 with one-bolt connections) have been tested. The full-scale tests on lattice systems were focused on the ultimate load of typical bracing members in lattice transmission towers. Therefore, the diagonals were realized as x-bracings with the tension and compression diagonal members bolted at their crossings, leading to a buckling support for the compression member and an eccentricity only on one end of the member. Current European design codes for lattice transmission towers (EN 50341-1 and EN 1993-3-1) are based on the recommendations developed in ECCS (1985).

Adluri et al. (1996) started a test series on 26 centrically loaded equal leg angles with hinged end supports at the University of Windsor (Canada). In the following years, two more testing campaigns have been carried out at that place, covering steel angles with two bolts (Haidar (1996), 197 tests) or one bolt (Shani 1998, 47 tests) in the connected leg.

20 tests on hot-rolled single steel angles with two-bolt connections and 13 tests in which the connected leg was welded to the support are presented in Schneider (2003).

Reininghaus et al. (2005) published 40 tests on single-angle columns with one-bolt connections. Residual stresses in hot-rolled steel angle sections are known to have rather low influence on the buckling resistance of these members, compared to their I-section counterparts. The traditional idealized distribution in ECCS (1976) – that can also be found in the American and the Chinese codes in similar form – has lately been compared with residual stress measurements of high-strength steel angles (Ban et al. (2012)) and large hot-rolled steel angles (Moze et al. (2014)).

Recently, a new design approach for centrically loaded hot-rolled steel angle columns, based on the direct strength method (DSM, e.g. Schafer (2008)), has been presented (Dinis et al. (2017)). The work is focused on equal-leg angle columns with fixed and pinned end supports with short-to-intermediate lengths showing flexural-torsional buckling modes.

Kettler et al. (2017) prepared about 300 of the above mentioned test results from literature with bolted connections in such a way that they could be compared with different design standards (same format as in Fig. 1, based on the slenderness ratio about the minimum axis  $\bar{\lambda}_y$ ). Additionally, the authors presented a systematic numerical parametric study highlighting the very high influence of the stiffness of the boundary condition (i.e. the end support of the gusset plate, rigid/hinged).

Although, the number of experimental tests in literature on the ultimate load of bolted single-angle steel members in compression is rather large, the authors are not aware of any tests systematically investigating the influence of different boundary conditions. Up to now, only the influence of one-bolt against two-bolt connections has been examined, disregarding the significant difference in the compression member capacity between clamped and hinged support of the gusset plate. Therefore, this paper presents 27 new experimental tests on bolted steel angles in compression with varying end support conditions.

## **2. Experimental tests on single-angle members in compression**

In total 27 experimental tests (14 with two-bolt connections and 13 with one-bolt connections) were conducted at Graz University of Technology. Most of the specimens were made of the frequently used European hot-rolled section L80x8 ( $b = 80$ ,  $t = 8\text{mm}$ ). Three specimens with two-bolt connections were fabricated of the larger L120x12 ( $b = 120$ ,  $t = 12\text{mm}$ ) section. Fig. 2 presents the examined specimens before testing. They have been arranged with one-bolt connection specimens on the left and two-bolt connection specimens on the right, both ordered by member length. The specimens were cut from five different long members, called A to E in Table 1 and Table 2. For the material testing, discussed in chapter 2.2, additional five short members have been cut from each of these long members. They can be seen on the top left in

Fig. 2. Fig. 3 shows the unloaded specimens after reaching the full member capacity in the tests. The remaining plastic deformations can clearly be identified.

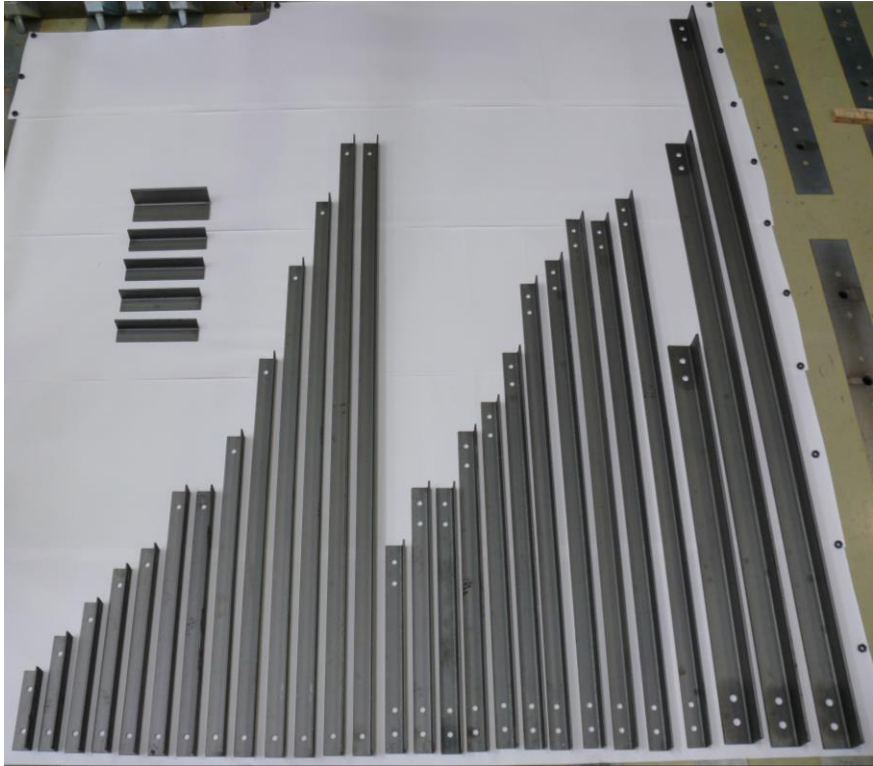


Figure 2: Test specimens before testing

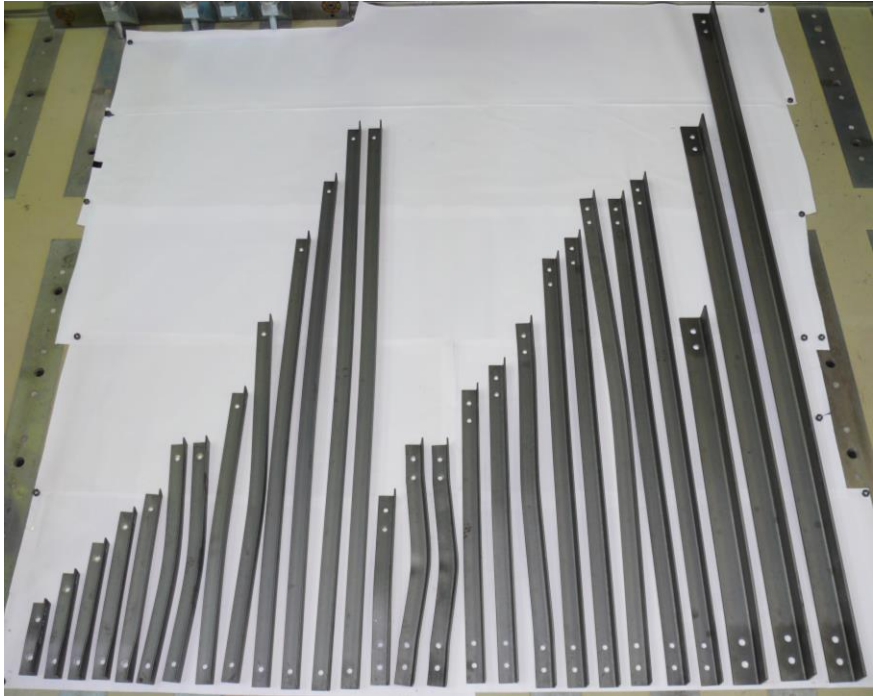


Figure 3: Test specimens after reaching the full member capacity in the tests

For the L80x8 sections M20 bolts of grade 10.9 were used, while M27 bolts of grade 10.9 were applied for the L120x12 sections. The bolts of four tests have been hand-tight (see Table 1), all other bolts have been preloaded (100%, based on EN 1993-1-8). Additionally, the real dimensions ( $b_{\text{mean}}$ ,  $t_{\text{mean}}$ ), the member length  $L_{\text{member}}$  and the system length  $L_{\text{sys}}$  (illustrated in Fig. 6) of all members and the three different types of boundary conditions are listed in the table. The different boundary conditions are: (i) Boundary condition 1 (BC1), a clamped support with all rotational degrees of freedom restraint at both member's ends; (ii) BC2, a knife edge support that allows only for rotations about the axis parallel to the connected leg; (iii) BC3, a fully hinged support with only the rotation about the longitudinal axis restraint. The individual end conditions are illustrated in Fig. 7.

Table 1: Summary of the testing program and measured geometric dimensions and imperfections

|    | Section | Bolts                    | Supports | $L_{\text{member}}$<br>[mm] | $L_{\text{sys}}^3$<br>[mm] | $b_{\text{mean}}$<br>[mm] | $t_{\text{mean}}$<br>[mm] | $e_{\text{imp}}$<br>[mm] | $L_{\text{sys}}/e_{\text{imp}}$<br>[-] |
|----|---------|--------------------------|----------|-----------------------------|----------------------------|---------------------------|---------------------------|--------------------------|--|
| A1 | 80x8    | 2x M20 10.9              | BC1      | 1140                        | 1180                       | 80.4                      | 8.2                       | 0.40                     | 2950                                   |
| A2 | 80x8    | 2x M20 10.9              | BC1      | 1820                        | 1860                       | 80.3                      | 8.1                       | 1.45                     | 1283                                   |
| A3 | 80x8    | 2x M20 10.9              | BC1      | 2630                        | 2670                       | 80.4                      | 8.3                       | 1.60                     | 1669                                   |
| A4 | 80x8    | 2x M20 10.9              | BC2      | 870                         | 1005                       | 80.3                      | 8.2                       | 0.25                     | 4020                                   |
| A5 | 80x8    | 2x M20 10.9              | BC2      | 1550                        | 1685                       | 80.3                      | 8.2                       | 1.15                     | 1465                                   |
| A6 | 80x8    | 2x M20 10.9              | BC2      | 2360                        | 2495                       | 80.3                      | 8.2                       | 1.45                     | 1721                                   |
| B1 | 80x8    | 2x M20 10.9              | BC3      | 1410                        | 1490                       | 79.5                      | 7.8                       | 0.65                     | 2292                                   |
| B2 | 80x8    | 2x M20 10.9              | BC3      | 2220                        | 2300                       | 79.5                      | 7.8                       | 1.35                     | 1704                                   |
| B3 | 80x8    | 2x M20 10.9              | BC3      | 2770                        | 2850                       | 79.5                      | 7.9                       | 2.10                     | 1357                                   |
| B4 | 80x8    | 1x M20 10.9              | BC1      | 1140                        | 1180                       | 79.4                      | 7.8                       | 0.35                     | 3371                                   |
| B5 | 80x8    | 1x M20 10.9              | BC1      | 1820                        | 1860                       | 79.5                      | 7.8                       | 1.15                     | 1617                                   |
| C1 | 80x8    | 1x M20 10.9              | BC1      | 3170                        | 3210                       | 79.4                      | 7.8                       | 1.10                     | 2918                                   |
| C2 | 80x8    | 1x M20 10.9              | BC2      | 870                         | 1005                       | 79.4                      | 7.8                       | 0.25                     | 4020                                   |
| C3 | 80x8    | 1x M20 10.9              | BC2      | 2360                        | 2495                       | 79.4                      | 7.8                       | 1.05                     | 2376                                   |
| C4 | 80x8    | 1x M20 10.9              | BC3      | 1410                        | 1490                       | 79.5                      | 7.8                       | 0.45                     | 3311                                   |
| C5 | 80x8    | 1x M20 10.9              | BC3      | 2770                        | 2850                       | 79.5                      | 7.9                       | 0.80                     | 3563                                   |
| D1 | 80x8    | 2x M20 10.9 <sup>1</sup> | BC1      | 1140                        | 1180                       | 79.4                      | 7.8                       | 0.60                     | 1967                                   |
| D2 | 80x8    | 2x M20 10.9 <sup>1</sup> | BC1      | 2630                        | 2670                       | 79.5                      | 7.9                       | 1.55                     | 1723                                   |
| D3 | 80x8    | 1x M20 10.9 <sup>1</sup> | BC1      | 1140                        | 1180                       | 79.5                      | 7.8                       | 0.45                     | 2622                                   |
| D4 | 80x8    | 1x M20 10.9 <sup>1</sup> | BC1      | 3170                        | 3210                       | 79.4                      | 7.9                       | 2.55                     | 1259                                   |
| D5 | 80x8    | 1x M20 10.9              | BC3      | 320                         | 400                        | 79.4                      | 7.8                       | 0.05                     | 8000                                   |
| D6 | 80x8    | 1x M20 10.9              | BC3      | 470                         | 550                        | 79.3                      | 7.9                       | 0.10                     | 5500                                   |
| D7 | 80x8    | 1x M20 10.9              | BC3      | 620                         | 700                        | 79.3                      | 7.8                       | 0.15                     | 4667                                   |
| D8 | 80x8    | 1x M20 10.9              | BC3      | 770                         | 850                        | 79.4                      | 7.8                       | 0.25                     | 3400                                   |
| E1 | 120x12  | 2x M27 10.9              | BC1      | 1850                        | 1890                       | 120.3                     | 12.0                      | 1.10                     | 1718                                   |
| E2 | 120x12  | 2x M27 10.9              | BC1      | 3170                        | 3210                       | 120.1                     | 12.0                      | 2.85                     | 1126                                   |
| E3 | 120x12  | 2x M27 10.9              | BC1      | 4200                        | 4240                       | 120.3                     | 12.0                      | 2.65                     | 1600                                   |

1. Indicated bolts were not preloaded, but only hand-tight
2. Note: BC1 = clamped support, BC2 = knife-edge support, BC3 = hinged support
3.  $L_{\text{sys,BC1}} = L_{\text{member}} + 40\text{mm}$ ,  $L_{\text{sys,BC2}} = L_{\text{member}} + 135\text{mm}$ ,  $L_{\text{sys,BC3}} = L_{\text{member}} + 80\text{mm}$

### 2.1 Cross-sectional dimensions and geometric imperfections

In order to be able to compare the test results with other tests from literature or with numerical calculations, it is necessary to gain information about the actual cross-sectional dimensions and geometric imperfections. Fig. 4 exemplarily shows the measurement of these parameters. The left picture shows the measurement of the wall thickness  $t$  with an electronic sliding caliper, while the right picture illustrates the determination of the bow imperfection  $e_{\text{imp}}$  about the minor axis (see Fig. 1) of the angle section with a thickness gauge (note that the steel foundation

beneath the angle section was mechanically milled to achieve a nearly perfect flat surface). The wall thickness  $t$  has been measured for each specimen on both member ends and twice for each angle leg. These eight thickness values have been averaged resulting in the mean thickness value  $t_{\text{mean}}$  in Table 1. The section width  $b$  has been measured on both specimen ends and for both legs, resulting in the mean width value  $b_{\text{mean}}$  in the Table 1.

The tabulated amplitude  $e_{\text{imp}}$  of the global bow imperfection about the minor axis is related to the system length  $L_{\text{sys}}$  of the member in the last column of Table 1. The comparison highlights the very small geometric imperfections of the investigated test specimens. Note that in Eurocode a maximum geometric imperfection of  $e_0 = L/750$  is tolerated. In total, measurements of local (angle leg deformations out of plane) and global (bow imperfections) geometric imperfections at 15 different positions have been conducted for each specimen. Since these values were all rather small, they have not been included in Table 1.

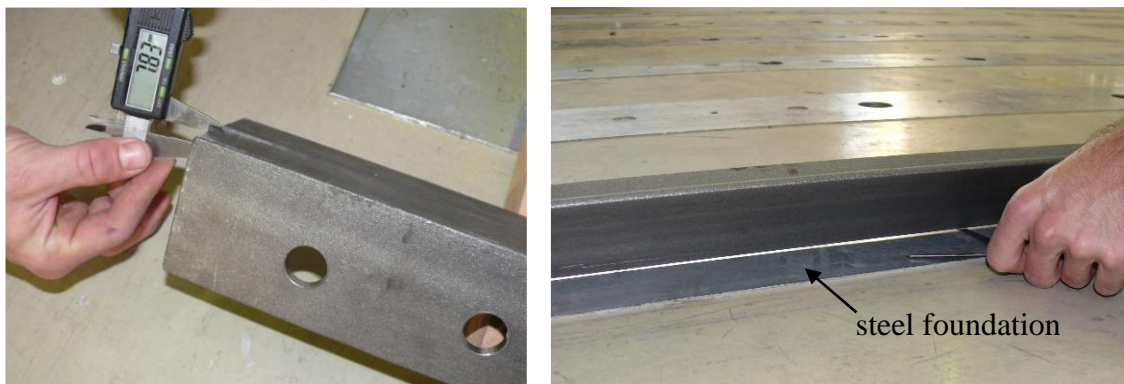


Figure 4: Measurement of cross-section dimensions and geometrical imperfections  $e_{\text{imp}}$

## 2.2 Material properties

Accompanying to the results of the member tests, material tests have been conducted. The five short sections in Fig. 2 were used for these tests. From every section, three tensile coupon specimens have been cut out. Two flat bar specimens from the angle legs and one round bar specimen from the corner region of the angle section, see Fig. 5. The tensile tests were performed in accordance with EN ISO 6892-1 with a loading rate of 2 mm/min for the flat bar and 1 mm/min for the round bar specimens. Fig. 5 also shows the tensile coupon specimens after testing.

The results of the material tests (i.e. the yield strength  $f_{y,\text{test}}$ , the tensile strength  $f_{u,\text{test}}$  and the Young's modulus  $E_{\text{test}}$ ) are summarized in Table 2. For further comparison, the yield strength  $f_{y,\text{test}}$  and the Young's modulus  $E_{\text{test}}$  have been averaged over each original section. This was realized via the definition of the three subareas A1 to A3, see Fig. 5 and Table 2. The measurement results were averaged, using the corresponding subareas as weight functions, resulting in the mean values  $f_{y,\text{mean}}$  and  $E_{\text{mean}}$  in Table 2. These two values have been used for further investigations.

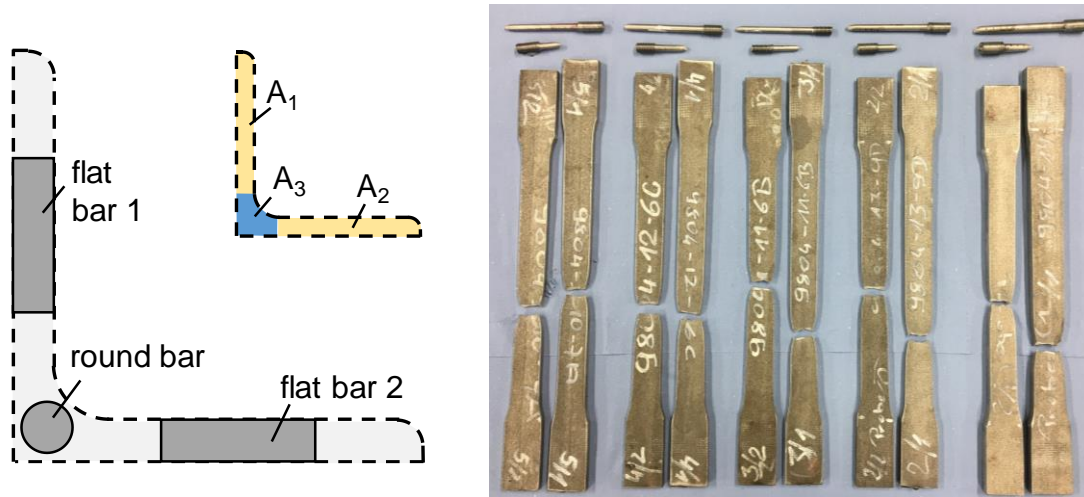


Figure 5: Tensile coupon specimens: location in section and defined subareas (left), specimens after testing (right)

Table 2: Table of results of tensile coupon tests

|   | Test No | Type      | $f_{y,test}$ [MPa] | $f_{u,test}$ [MPa] | $E_{test}$ [MPa] | A1 [mm <sup>2</sup> ] | A2 [mm <sup>2</sup> ] | A3 [mm <sup>2</sup> ] | $E_{mean}$ [MPa] | $f_{y,mean}$ [MPa] |
|---|---------|-----------|--------------------|--------------------|------------------|-----------------------|-----------------------|-----------------------|------------------|--------------------|
| A | 5/1     | flat bar  | 297                | 396                | 210 100          |                       |                       |                       | 212368           | 289.9              |
|   | 5/2     | flat bar  | 287                | 393                | 204 600          | 502                   | 506                   | 250                   |                  |                    |
|   | 5       | round bar | 282                | 396                | 232 600          |                       |                       |                       |                  |                    |
| B | 3/1     | flat bar  | 322                | 468                | 201 100          |                       |                       |                       | 199458           | 326.8              |
|   | 3/2     | flat bar  | 325                | 465                | 204 100          | 477                   | 479                   | 238                   |                  |                    |
|   | 3       | round bar | 341                | 471                | 186 800          |                       |                       |                       |                  |                    |
| C | 4/1     | flat bar  | 326                | 468                | 208 100          |                       |                       |                       | 209284           | 333.9              |
|   | 4/2     | flat bar  | 326                | 466                | 206 300          | 475                   | 480                   | 237                   |                  |                    |
|   | 4       | round bar | 367                | 478                | 217 700          |                       |                       |                       |                  |                    |
| D | 2/1     | flat bar  | 319                | 460                | 197 000          |                       |                       |                       | 194818           | 322.4              |
|   | 2/2     | flat bar  | 316                | 460                | 184 800          | 474                   | 479                   | 237                   |                  |                    |
|   | 2       | round bar | 341                | 475                | 210 700          |                       |                       |                       |                  |                    |
| E | 1/1     | flat bar  | 296                | 459                | 185 300          |                       |                       |                       | 192156           | 299.3              |
|   | 1/2     | flat bar  | 304                | 470                | 195 700          | 1 141                 | 1 132                 | 486                   |                  |                    |
|   | 1       | round bar | 296                | 469                | 200 000          |                       |                       |                       |                  |                    |

### 2.3 Member tests

The main part of the test series consisted of the 27 member buckling tests. Specimens with one or two bolts in the connected web were investigated, with the specified connection details given in Fig. 6. The three different boundary conditions are illustrated in Fig. 7 (BC1: clamped support, BC2: knife edge support, BC3: hinged support). For all boundary conditions, gusset plates with a thickness of 25 mm have been used, see Fig 6.

The rather high thickness of the gusset plate was chosen to get capacities that could be interpreted as upper limits for BC1, the clamped support. For BC2 and BC3 the thickness of the gusset plate is of minor importance. The gusset plates were welded to endplates of 20 mm thickness. These endplates were directly fixed with the rigid support block at the bottom and the rigid load cell at the hydraulic jack at the top for BC1. To allow for the rotations about the axis parallel to the connected leg (BC2), additional construction elements were attached to the end plates of the specimens. At the top, a conventional centering bar was used, while a specific

device with a roller has been used at the bottom, see Fig. 7. BC3, the hinged support, was realized via spherical pressure plates at the top and the bottom that allowed for nearly free rotation about all three axes. Although the hinged construction was properly lubricated, some friction occurred resulting in a certain rotational stiffness. This phenomenon will be further discussed in chapter 3, where the results of the member tests are presented.

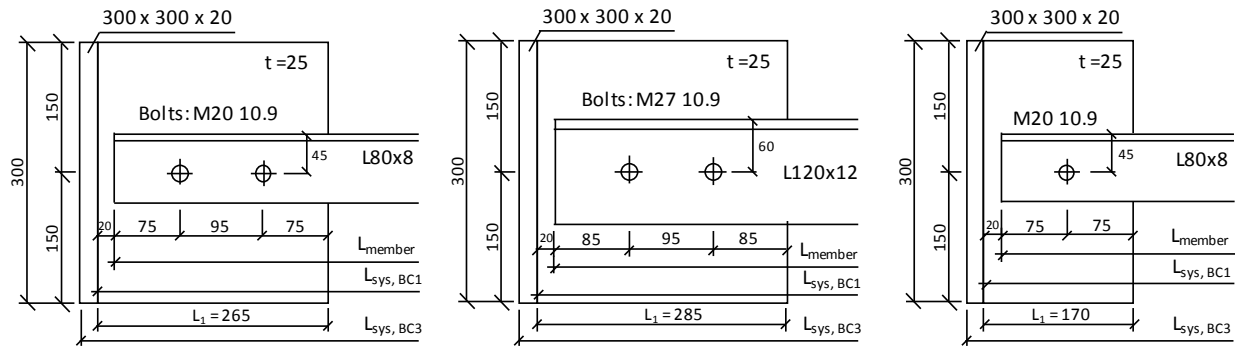


Figure 6: Details of the bolted connections at both member ends for one and two bolts

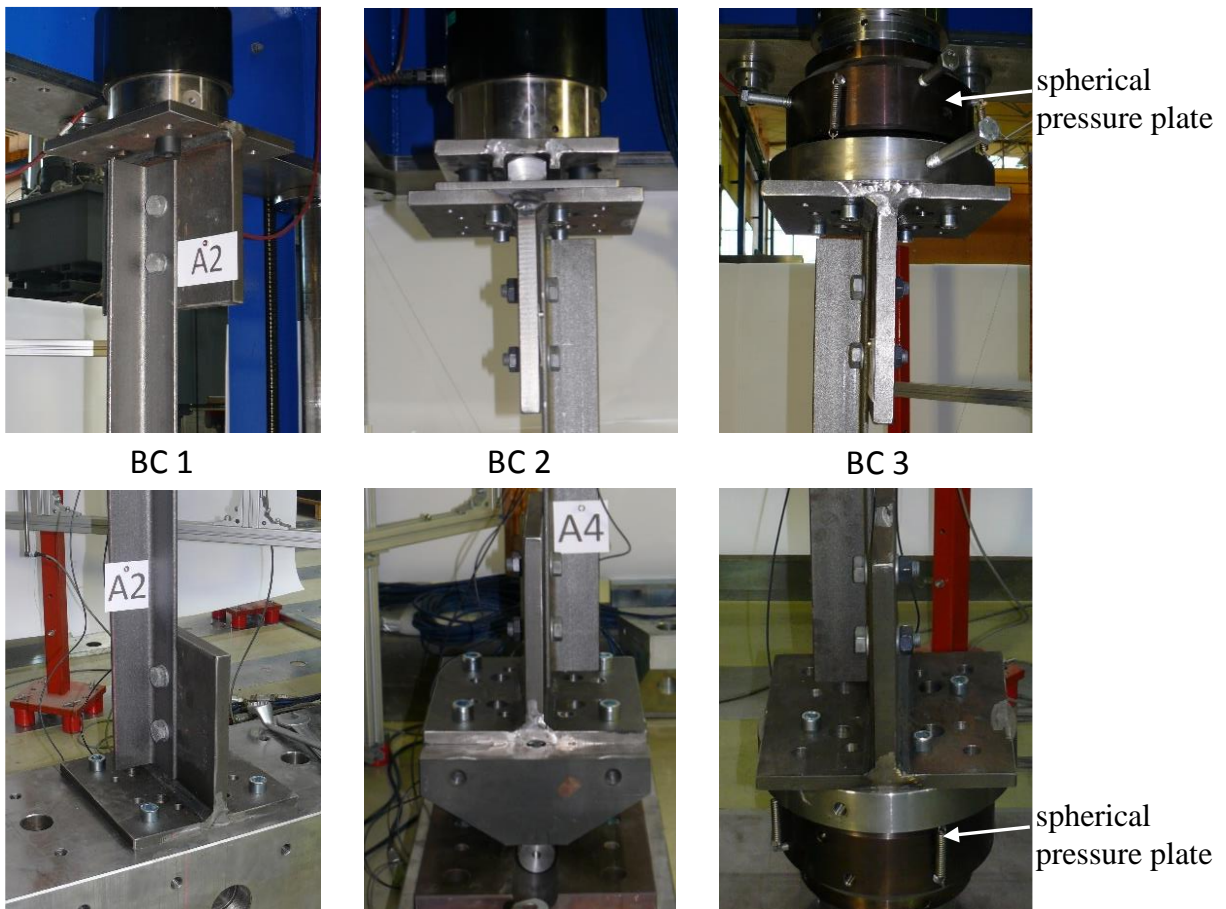


Figure 7: Investigated boundary conditions: BC1 clamped support, BC2 knife edge support, BC3 hinged support

Fig. 8 illustrates the measuring devices at midspan of the specimens. The strains in axial direction were measured with three DD1 strain gauges (numbered with 10, 11 and 12 in the

picture). The three translational deformations and the rotation about the longitudinal axis of the mid-cross-section were indirectly measured with four inductive displacement transducers ( $w_1 - w_3$  and  $w_\varphi$  in Fig. 8). The four strings connecting the specimen with the displacement transducers can also be seen in Fig. 8. The effective deformations of the mid-section (all translations and the rotation about the longitudinal axis) could then be calculated from the four measured values.

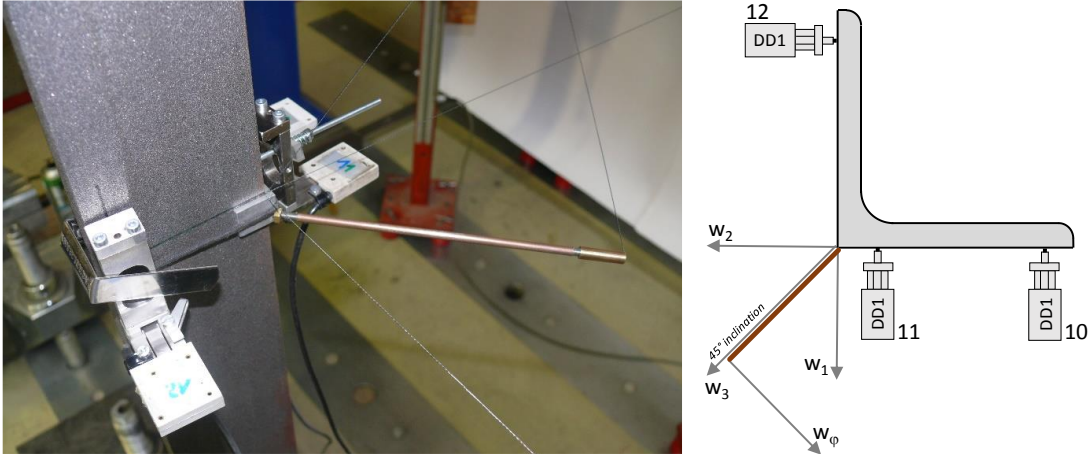


Figure 8: Measuring devices at midspan of the angle member

Fig. 9 exemplarily shows the member buckling tests for two angle sections with member length  $L_{\text{member}} = 1820\text{mm}$ . Specimen A2 (left picture) is loaded via two-bolt connections, while specimen B5 (right picture) features one-bolt connections. All bolts have been preloaded. The boundary condition for both tests is BC1 (clamped support). By comparing the deformed shape of both tests, the well-known characteristic difference in the load carrying behavior between one- and two-bolt connections can be verified. The member ends are kept vertically straight for specimen A2, because of the presence of the two bolts in the connected leg. The single preloaded bolt in the connected leg of specimen B5, although fully preloaded, is obviously not enough to prevent the end-rotation of the member. It is worth noting that the steel surface of the gusset plate and the angle section were sandblasted resulting in rather favorable friction conditions. Therefore, it can be assumed that this end-rotation will also occur in real structures.

### 3. Results

This chapter summarizes the main results of the experimental test campaign on single steel angles in compression with varying end support conditions and one- or two-bolt connections at the end. Table 3 shows the calculation of the nominal fully plastic axial resistance  $N_{pl}$  of the section (Eq. 1) and the elastic critical buckling force  $N_{cr}$  for buckling about the minor axis. For this, the actual geometric values of the cross-section area  $A$  and the second moment of area  $I_v$  about the minor axis – both based on the measured geometric parameters for each individual angle member – have been used.

$$N_{pl} = A \cdot f_{y,mean} \quad (1)$$

The corresponding values for the averaged Young's modulus  $E_{\text{mean}}$  and yield strength  $f_{y,mean}$  are also tabulated, based on the calculated mean values given in Table 2. Note that  $N_{cr}$  has always

been calculated based on the system length  $L_{sys}$  of the member to give a better overview. For the values of  $L_{sys}$  see Table 1. The non-dimensional slenderness  $\bar{\lambda}_v$  was calculated with Eq. 2:

$$\bar{\lambda}_v = \sqrt{\frac{N_{pl}}{N_{cr}}} \quad (2)$$



Figure 9: Member buckling tests for specimen A2 (two-bolt connection) and specimen B5 (one-bolt connection)

Table 3: Summary of experimental ultimate loads and corresponding slenderness values

|    | A     | $I_v$              | $E_{\text{mean}}$  | $f_{y,\text{mean}}$  | $N_{\text{pl}}$      | $N_{\text{cr}}^1$ | $\bar{\lambda}_v$ | $N_R$ | $N_R / N_{\text{pl}}$ |      |
|----|-------|--------------------|--------------------|----------------------|----------------------|-------------------|-------------------|-------|-----------------------|------|
|    | Bolts | [cm <sup>2</sup> ] | [cm <sup>4</sup> ] | [N/mm <sup>2</sup> ] | [N/mm <sup>2</sup> ] | [kN]              | [kN]              | [-]   | [kN]                  | [-]  |
| A1 | 2     | 12.6               | 31.0               | 212368               | 289.9                | 365.9             | 466.8             | 0.89  | 261.1                 | 0.71 |
| A2 | 2     | 12.5               | 30.7               | 212368               | 289.9                | 362.9             | 186.1             | 1.40  | 238.8                 | 0.66 |
| A3 | 2     | 12.7               | 31.2               | 212368               | 289.9                | 368.0             | 91.7              | 2.00  | 215.4                 | 0.59 |
| A4 | 2     | 12.6               | 30.8               | 212368               | 289.9                | 364.3             | 639.3             | 0.75  | 156.8                 | 0.43 |
| A5 | 2     | 12.5               | 30.7               | 212368               | 289.9                | 363.1             | 226.4             | 1.27  | 117.8                 | 0.32 |
| A6 | 2     | 12.6               | 31.0               | 212368               | 289.9                | 366.0             | 104.2             | 1.87  | 71.8                  | 0.20 |
| B1 | 2     | 11.9               | 28.6               | 199458               | 326.8                | 397.2             | 253.7             | 1.25  | 148.0                 | 0.37 |
| B2 | 2     | 11.9               | 28.7               | 199458               | 326.8                | 397.5             | 106.7             | 1.93  | 86.4                  | 0.22 |
| B3 | 2     | 12.0               | 28.8               | 199458               | 326.8                | 399.7             | 69.8              | 2.39  | 61.0                  | 0.15 |
| B4 | 1     | 11.9               | 28.6               | 199458               | 326.8                | 398.0             | 404.4             | 0.99  | 162.9                 | 0.41 |
| B5 | 1     | 12.0               | 28.7               | 199458               | 326.8                | 399.0             | 163.5             | 1.56  | 132.1                 | 0.33 |
| C1 | 1     | 11.9               | 28.6               | 209284               | 333.9                | 390.0             | 57.4              | 2.61  | 98.4                  | 0.25 |
| C2 | 1     | 11.9               | 28.5               | 209284               | 333.9                | 389.3             | 583.8             | 0.82  | 120.9                 | 0.31 |
| C3 | 1     | 11.9               | 28.7               | 209284               | 333.9                | 390.3             | 95.1              | 2.03  | 66.0                  | 0.17 |
| C4 | 1     | 11.9               | 28.7               | 209284               | 333.9                | 390.1             | 267.2             | 1.21  | 131.0                 | 0.34 |
| C5 | 1     | 12.0               | 28.9               | 209284               | 333.9                | 392.4             | 73.4              | 2.31  | 62.6                  | 0.16 |
| D1 | 2     | 11.9               | 28.6               | 194818               | 322.4                | 383.9             | 394.9             | 0.99  | 260.2                 | 0.68 |
| D2 | 2     | 12.0               | 28.7               | 194818               | 322.4                | 385.7             | 77.5              | 2.23  | 177.5                 | 0.46 |
| D3 | 1     | 11.9               | 28.7               | 194818               | 322.4                | 384.8             | 396.6             | 0.99  | 154.8                 | 0.40 |
| D4 | 1     | 12.0               | 28.8               | 194818               | 322.4                | 386.2             | 53.7              | 2.68  | 73.1                  | 0.19 |
| D5 | 1     | 11.8               | 28.3               | 194818               | 322.4                | 381.2             | 3406.6            | 0.33  | 145.5                 | 0.38 |
| D6 | 1     | 11.9               | 28.6               | 194818               | 322.4                | 385.1             | 1818.0            | 0.46  | 151.0                 | 0.39 |
| D7 | 1     | 11.9               | 28.4               | 194818               | 322.4                | 382.1             | 1113.3            | 0.59  | 148.8                 | 0.39 |
| D8 | 1     | 11.9               | 28.6               | 194818               | 322.4                | 383.8             | 760.2             | 0.71  | 145.0                 | 0.38 |
| E1 | 2     | 27.7               | 153.0              | 192156               | 299.3                | 827.9             | 812.1             | 1.01  | 488.4                 | 0.59 |
| E2 | 2     | 27.6               | 152.2              | 192156               | 299.3                | 826.5             | 280.1             | 1.72  | 357.2                 | 0.43 |
| E3 | 2     | 27.6               | 152.7              | 192156               | 299.3                | 826.3             | 161.1             | 2.27  | 267.1                 | 0.32 |

1. The values  $N_{\text{cr}}$  have been calculated with  $L_{\text{sys}}$

It is evident, that the effects of the boundary conditions (BC1 to BC3) and also the bending stiffness of the gusset plates can be considered in the calculation of  $N_{\text{cr}}$ . This was also done by the authors, but gives no significant changes for the interpretation of the results.

Finally, Table 3 summarizes the achieved ultimate axial compression forces  $N_R$  for all experiments and relates these values to the full plastic axial resistance  $N_{\text{pl}}$  in the last column.

In Fig. 10-12 the test results are compared with the relevant European design standards by means of  $N_R/N_{\text{pl}}$  over  $\bar{\lambda}_v$  diagrams. Additionally, preliminary numerical calculations that already have been published by the authors (Kettler et al. (2017)) are presented in the figures. Note that these finite element calculations have been carried out with equivalent geometric imperfections with an amplitude of  $e_0 = L_{\text{sys}}/300$ .

Fig. 10 shows the results for the three experimental tests on L120x12 sections with two bolts in the connected leg. The investigated boundary condition is BC1 (clamped support). The very good agreement between the test results and the numerical calculations is evident. It can also be verified that all design codes yield conservative predictions for the member buckling resistance for  $\bar{\lambda}_v \geq 1.0$ . For smaller slenderness values the design codes seem to give too favorable estimations for the studied angle members with eccentricities on both ends.

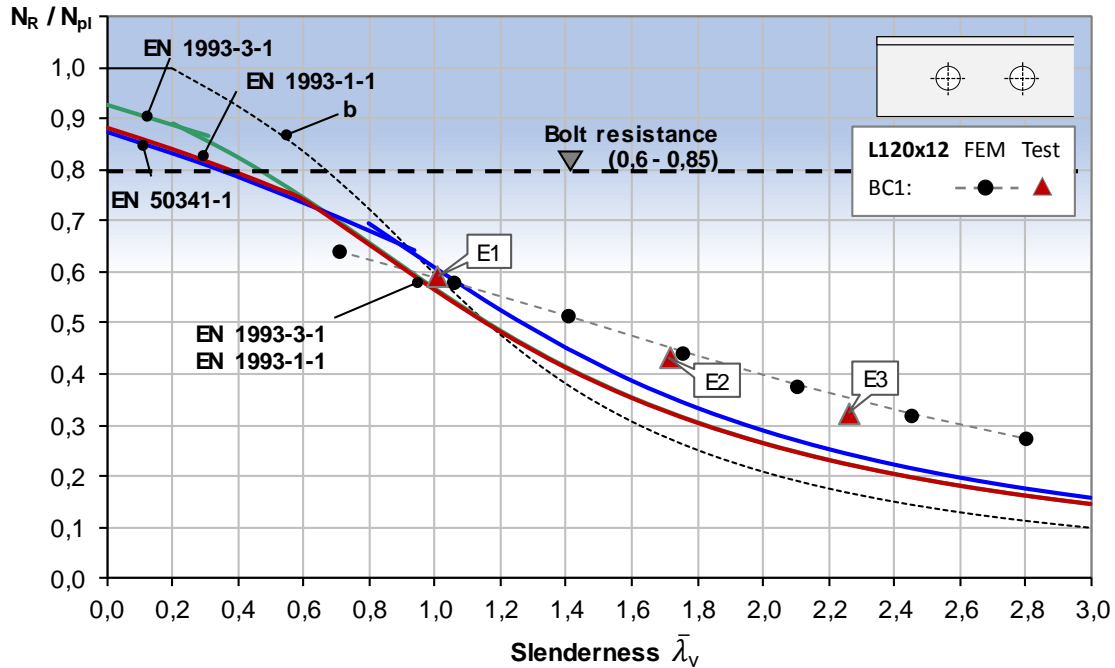


Figure 10: Comparison of L120x12 test results for two-bolt connections with design standards and numerical calculations – clamped end supports (BC1)

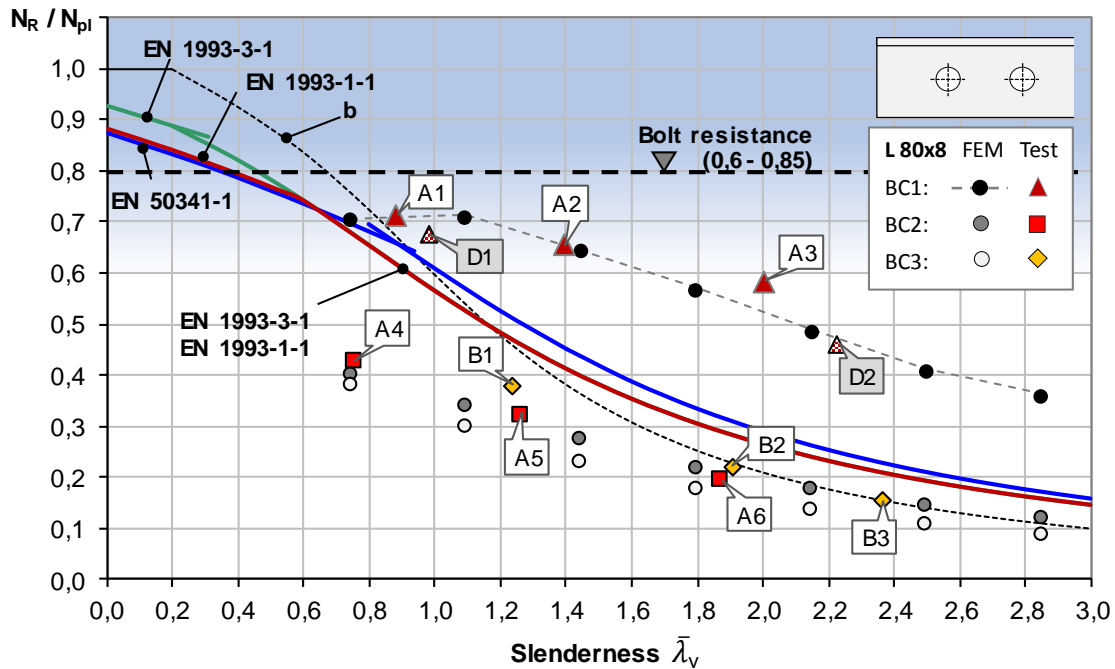


Figure 11: Comparison of L80x8 test results for two-bolt connections with design standards and numerical calculations – all boundary conditions

Fig. 11 presents the results of the 11 tests on L80x8 sections with two-bolt connections. The experimental tests comprise all three different boundary conditions. The tests for BC1 and BC2 (knife edge support) show very good agreement with the preliminary finite element calculations.

The experimental tests on BC3 (hinged support) gave higher resistances than the tests for BC2. The reason for this lies in the fact that the constructional element that provided more or less free rotation about all axes provided a certain rotational stiffness for the specimens. Since the buckling resistance of single-angle members is very sensitive to variations of the rotational stiffness at the member's ends, the results are even higher than for BC2. The illustrated numerical results for BC3 indicate the theoretical behavior for angle sections with fully hinged support. Interestingly, the difference in resistance between BC1 and BC2 is much higher than between BC2 and BC3. Generally, the high influence of different boundary conditions is evident.

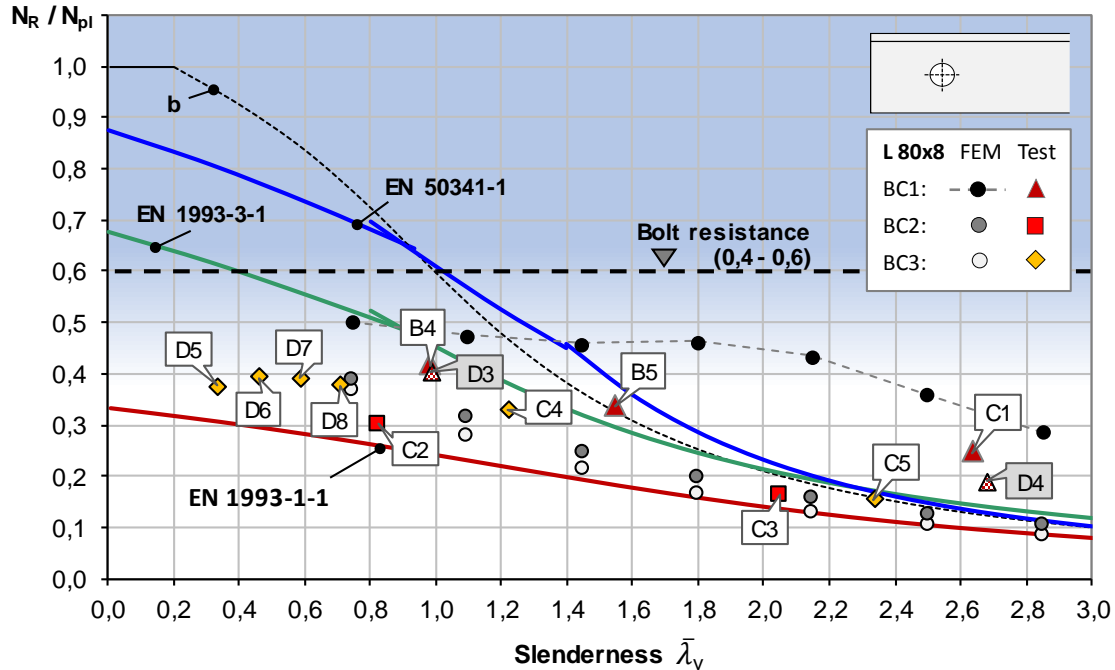


Figure 12: Comparison of L80x8 test results for one-bolt connections with design standards and numerical calculations – all boundary conditions

By comparing the results for BC2 and BC3 in Fig. 11 and Fig. 12 with each other, it can be verified that the buckling resistance is more or less the same for the cases with one bolt and with two bolts in the connected leg.

Typically, all bolts were preloaded. Some additional tests with BC1 in Fig. 11 and Fig. 12 (D1-D4) were conducted with hand-tight bolts in order to estimate the influence of preloading on the ultimate load. The results indicate that preloading in fact increases the member buckling resistance, but that the influence of different boundary conditions is more important than that.

#### 4. Conclusions

The results of the conducted test series on single steel angles in compression with bolted connections and varying end support conditions provide the following conclusions:

The member buckling resistances with boundary conditions BC2 (knife edge support) and BC3 (hinged support) are more or less the same for the cases with one bolt and with two bolts in the connected leg.

The well-known difference in the load carrying behavior between one-bolt and two-bolt connections could be verified only for BC1 (clamped support).

Single-angle members with two bolts in the connected leg exhibit a significant increase of the ultimate compressive strength for BC1, compared to BC2 and BC3. Therefore, current activities by the authors are in progress in order to generate appropriate stiffness values for gusset plates, based on practical applications, and to further study the real compression behavior of bolted angles in compression in more detail.

## References

- AISC 360-16. "Specification for Structural Steel Buildings." ANSI, Chicago, 2016.
- Ban, H., Shi, G., Shi, Y., Wang, Y. (2012). "Residual stress tests of high-strength steel equal angles." *Journal of Structural Engineering*, 138 (12), 1446-1454.
- Adluri, S.M.R., Madugula, M.K.S. (1996). "Flexural buckling of steel angles – Experimental Investigation." *Journal of Structural Engineering*, 122 (3), 309-317.
- C.I.G.R.E. (1974). Study Committee No. 22, Test report. "Buckling tests on crossed diagonals in lattice towers", Electra Cigré/No. 38.
- CSA S16-14. "Design of steel structures." CSA Group, Toronto, 2014.
- Dinis, P.B., Camotim, D., Vieira, L. (2017), "DSM design approach for hot rolled steel angle columns." *Proceedings of Eurosteel 2017*, 3781-3790. doi:10.1002/cepa.434.
- ECCS (1976). TC8 Stability, "Manual on stability of steel structures." No 22.
- ECCS (1985). TC8 Stability, "Recommendations for angles in lattice transmission towers." No 39.
- EN 1993-1-1. "Eurocode 3: Design of steel structures – Part 1-1: General rules and rules for buildings." CEN, Brussels, 2005.
- EN 1993-1-8. "Eurocode 3: Design of steel structures – Part 1-8: Design of joints." CEN, Brussels, 2005.
- EN 1993-3-1. "Eurocode 3: Design of steel structures – Part 3-1: Towers, masts and chimneys – Towers and masts". CEN, Brussels, 2006.
- EN 50341-1. "Overhead electrical lines exceeding AC 45 kV – Part 1: General requirements – Common specifications". CENELEC, 2001.
- EN ISO 6892-1. "Metallic materials – Tensile testing – Part 1: Method of test at room temperature", 2009.
- Haidar, R. (1996). "Compressive strength of steel single angles loaded through two-bolts in one leg." *Master thesis*, University of Windsor.
- Kettler, M., Taras, A., Unterweger, H. (2017). "Member capacity of bolted steel angles in compression: Influence of realistic end supports." *Journal of constructional steel research*, 130, 22-35.
- Moze, P., Cajot, L.-G., Sinur, F., Rejec, K., Beg, D. (2014) "Residual stress distribution of large steel equal leg angles." *Engineering Structures*, 71, 35-47.
- Reininghaus, M., Skottke, M. (2005). "Druckbeanspruchte Winkelprofile mit Ein-Schrauben-Anschluß." *Stahlbau* 74 (7), 534-538.
- Schafer, B.W. (2008). „Review: The Direct Strength Method of cold-formed steel member design.” *Journal of Constructional Steel Research*, 64, 766-778.
- Schneider, R.W. (2003). "Beitrag zur Bemessung von druckbeanspruchten Einzelwinkeln unter Berücksichtigung der Anschlusseigenschaften." *PhD thesis*, RWTH Aachen, Shaker Verlag (No. 48).
- Shani, M.A. (1998). „Compressive strength of eccentrically loaded steel angles.” *Master thesis*, University of Windsor.